Kungl. Tekniska Högskolan
Institutionen för Energiteknik
100 44 Stockholm

http://www.energy.kth.se

Properties of New Low GWP Refrigerants

Slutrapport till projekt nr. P24 inom energimyndighetens program Effsys 2

Contents

List of figures

List of tables

P24 – Properties of New Low GWP Refrigerants

Sad Jarall Ph. D
ETT, Energiteknik, KTH, Stockholm

Abstract

Thermo-physical properties of low global warming potential (GWP) refrigerants were obtained to study and compare their performance with R22 and R134a. Theoretical cycle data, pressure drop, and heat transfer of HFO-1234yf were calculated and compared with those of R134a. Drop-in tests were carried out using two refrigeration units of plate heat exchangers: one for R22 and R290, and the other for R134a and HFO-1234yf. The results were compared to those concluded theoretical.

(**Sammanfattning**: Termodynamiska egenskaper för köldmedier med låg påverkan på den globala uppvärmningen (GWP) har insamlats för att jämföras med R22 och R134a. Teoretiska cykeldata, tryckfall och värmeöverföringstal för HFO-1234yf har beräknats och jämförts med motsvarande för R134a. *Drop-in* tester utfördes i två olika kylsystem med plattvärmeväxlare; ett för R22 och R290 samt ett för R134a och HFO-1234yf. De experimentella värdena utvärderades sedan mot de teoretiskt framtagna.)

Nomenclature

COP_{2d} Coefficient of performance of cycle
h_1' Condenser outlet enthalpy with no subcooling, kJ/kg
$h_{1k,is}$ Outlet enthalpy after isentropic compression of superheated vapor, kJ/kg
$h_{1k,is,o}$ Outlet enthalpy after isentropic compression of saturated vapor, kJ/kg
h''_{2k} Compressor inlet enthalpy of saturated vapor, kJ/kg
h_{2k} Compressor inlet enthalpy of superheated vapor, kJ/kg
H heat transfer coefficient
m_r Measured refrigerant mass flow rate, kg/s
m_w Water mass flow rate, kg/s
p_1 Condenser pressure, bar
p_2 Evaporator pressure, bar
p_{red} Reduced pressure = actual pressure/critical pressure
$Q_{1(r)}$ Condenser effect based on the refrigerant data, kW
$Q_{1(w)}$ Condenser effect based on the water data, kW
$Q_{2(r)}$ Evaporator effect based on the refrigerant data, kW
Q_{2v} Volumetric evaporator effect based on the refrigerant data, kJ/m^3
s Entropy, kJ/kg K
T_1, T_{1sat} Condenser saturation temperature, °C
$T_{1\,(in)}$ Condenser inlet temperature, °C
$T_{1\,(out)}$ Condenser outlet temperature, °C
T''_1 Condenser outlet temperature of saturated liquid, °C

T_2, T_{2sat} Evaporator saturation temperature, °C
T_{1kis} Compressor discharge temperature, °C
T_{2k} Copressor inlet temperature, °C
$T_{b(in)}$ Evaporator brine inlet temperature, °C
$T_{b(out)}$ Evaporator brine outlet temperature, °C
T_{ex} Temperature before the expansion valve, °C
T_s Condenser outlet temperature of subcooled liquid, °C
$T_{w(in)}$ Condenser water inlet temperature, °C
$T_{w(out)}$ Condenser water outlet temperature, °C
T_∞ Room temperature, °C
UA Overall heat transfer coefficient multiplied by the surface area, kW/°C
v Specific volume at compressor inlet, m^3/kg
Wv *Volumetric compressor work*, kJ/m^3
η_{cd} Cycle Carnot efficiency
Δp pressure drop (bar)

Introduction

The influence of fluorocarbon refrigerants on the global warming has prompted countries throughout the world to pass legislation preventing or phasing out the use of such refrigerants. In EU regulations have already been enacted to replace R134a in mobile air conditioning systems by a new low global warming potential (GWP) refrigerant, such as HFO-1234yf which has very similar thermodynamic properties as R134a in comparison to other environmentally less harmful candidates.

The purpose of this project is to collect information about alternative low GWP refrigerants, such as HFO-1234yf, R152a, and propane (R290), and investigate the feasibility of using them as replacements for previously used refrigerants. The selected refrigerants have the advantages of providing the same cooling effects, efficiencies, durability, and other performance factors as the original refrigerants do. No modifications are necessarily needed to the existing system. R290 may replace R22 in refrigeration installations with low evaporation temperature if safety measurements are to be considered due to its high flammability. R152a or HFO-1234yf may replace R134a in small, low pressure refrigeration units. HFO-1234yf is favorable due to its milder toxicity and flammability in comparison to R152a.

Evaluation of alternative refrigerant with low GWP

When selecting low GWP refrigerant, the first thing to investigate is its vapor pressure curve. It has to be similar to that of the original refrigerant if the original compressor is to be used, as fluids with similar vapor pressure curves will give similar capacities and require similar size of the compressor motor. Fig. 1 presents the saturation pressure vs. temperature of HFO-1234yf, R290, R152a, R717 as well as R134a and R22.

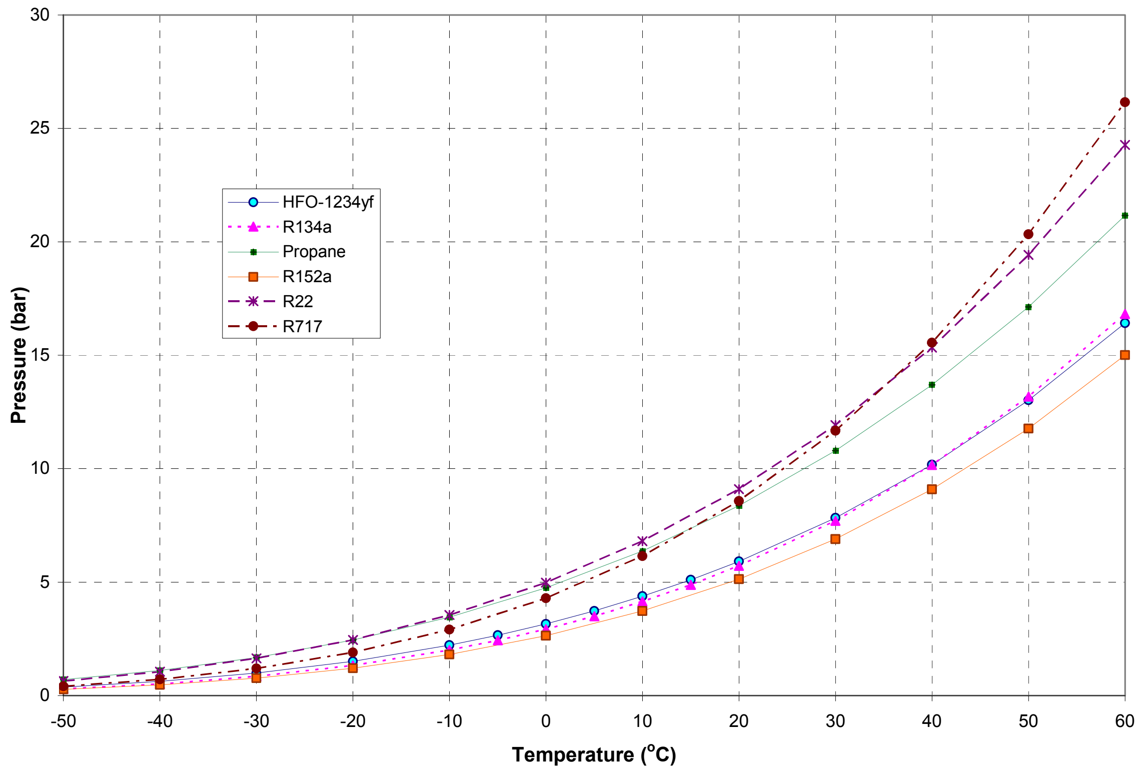

Fig. 1 Saturation pressure vs temperature

The figure shows that at the same temperatures R290 has the same or lower pressures than that of R22. At condensing temperature of 40 °C R290 has 10.7% less pressure than that of R22. Ammonia has similar pressure curve to R22 and from this respect it can be used as an alternative to R22. Yet, it is less favorable than propane as a replacement. It reacts with copper and bronze in the presence of a little moisture which demands the replacement of copper and bronze parts of the system with iron and steel parts. It has a high latent heat but low density. It is also irritating to breathe, somewhat flammable, and with the proper proportions of air may form an explosive mixture, although such an incident is rarely happened.

HFO-1234yf has similar vapor pressure curve as that of R134a, while R152a has lower pressure than these two refrigerants. However, HFO-1234yf is considered more frequently than R152a as a replacement for R134a as it poses less toxicity and flammability.

The refrigerants cooling, or heating, capacities that can be achieved with a given compressor and a given swept volume rate can easily be calculated in detail. Comparison between the refrigeration capacities for different refrigerants can be done by comparing the theoretical volumetric refrigerating capacity at defined evaporation and condensation temperatures. Fig. 2 shows the theoretical volumetric refrigerating capacities of different refrigerants versus the evaporation temperatures at condensation temperature of 40 ^{o}C and no superheating or subcooling.

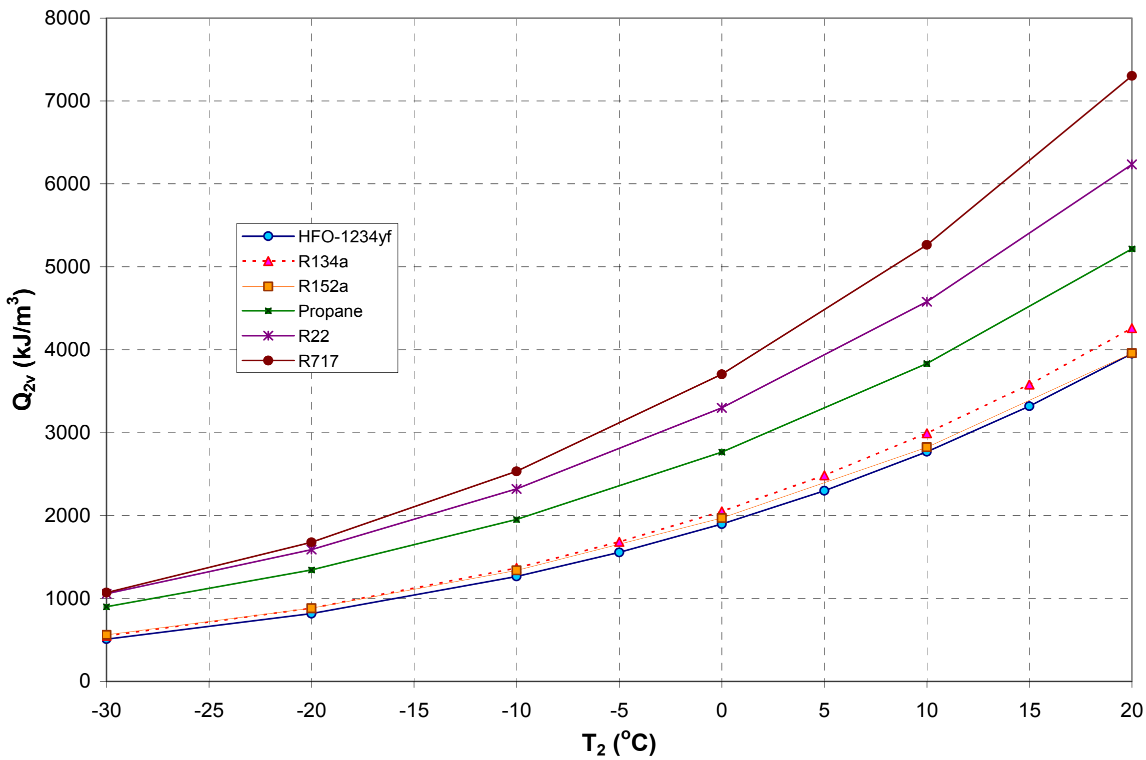

Fig. 2 Volumetric refrigerating effect vs. evaporation temperature at T_1 = 40 °C and no superheating or subcooling

The figure indicates that propane has less cooling capacity than R22 by 14.8% and 16.3% at evaporating temperature of -30 and 20°C, respectively. It also shows that HFO-1234yf has less volumetric cooling effect than R134a by 7.2%. At condensing temperature of 50°C the percentage of propane increases by approximately 2% while that of HFO-1234yf increases by 3%.

Drop-in tests for some different standard conditions performed at KTH lab using a refrigeration unit designed originally for R22 gave the results shown in table 1 below.

Table 1 Experimental data for drop-in tests at standard conditions

T_1 (°C)	T_2 (°C)	Super heat (°C)	Q_2 R22 (kW)	Q_2 R290 (kW)
54.5	7.2	22.8	1.647	1.587
40	-5	10	1.137	1.081
55	-12	10	0.678	0.621

The experimental data show less difference in the cooling effects than that indicated by Fig. 2 due to the influence of the superheat.

HFO-1234yf h-log(p)-diagram

HFO-1234yf ph-diagram is drawn using RefProp with reference state of *h* = 200 kJ/kg and *s* = 1 kJ/kg.K for saturated liquid at 0 °C. The density data are converted to specific volume data.

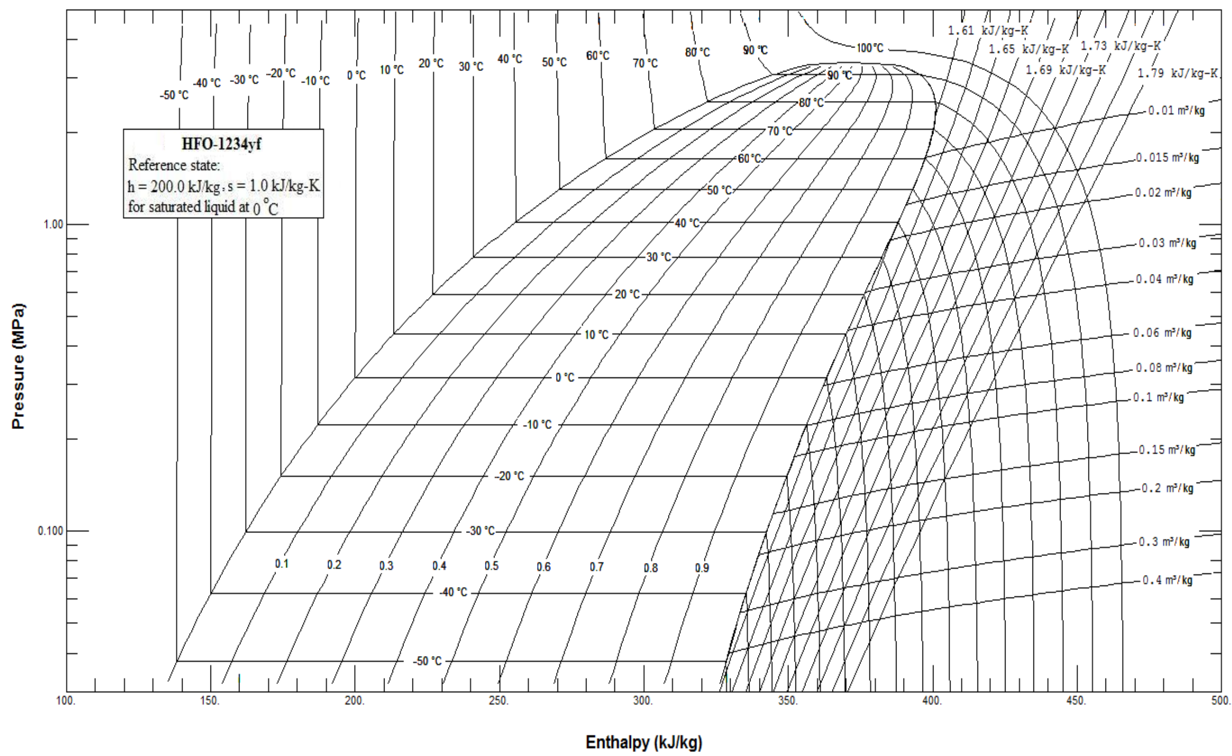

Fig. 3 Pressure enthalpy diagram of HFO-1234yf

HFO-1234yf cycle data

Cycle data are calculated, based on fluid properties taken from RefProp, for the theoretical cycle with isentropic compression and no subcooling of liquid or superheating of vapor. The data can be used to predict the basic performance of a new refrigerant and compare it to other known refrigerants. Influence of subcooling and superheating on the calculated volumetric cooling effect and the coefficient of performance is presented in the form of the factors y_1, y_2, y_3, and y_4, which are defined as:

y_1 (factor defining the influence of (external) subcooling on Q_{2v} and COP_{2d})

$$= (\frac{h''_{2k} - h_s}{h''_{2k} - h'_1} - 1) \cdot \frac{100}{T_1 - T_s}$$

y_2 (factor defining the influence of the internal superheat on Q_{2v})

$$= (\frac{h_{2k} - h'_1}{v_{2k}} \cdot \frac{v''_{2k}}{h''_{2k} - h'_1} - 1) \cdot \frac{100}{T_{2k} - T_2}$$

y_3 (factor defining the influence of the internal superheat on COP_{2d})

$$= (\frac{h_{2k} - h'_1}{h_{1k,is} - h_{2k}} \cdot \frac{h_{1k,is,o} - h''_{2k}}{h''_{2k} - h'_1} - 1) \cdot \frac{100}{T_{2k} - T_2}$$

y_4 (factor defining the influence of the external superheat on COP_{2d})

$$= (\frac{h_{1k,is,o} - h''_{2k}}{h_{1k,is} - h_{2k}} - 1) \cdot \frac{100}{T_{2k} - T_2}$$

Table 2 HFO-1234yf cycle data

T_1 (°C)	T_2 (°C)	p_1 (bar)	p_2 (bar)	p_1/p_2	T_{1kis}(°C)	Q_{2v} (kJ/m^3)	w_v (kJ/m^3)	COP_{2d}	η_{cd}	y_1 (%per°C)	y_2 (%per°C)	y_3 (%per°C)	y_4 (%per°C)
-20	-50	1.512	0.376	4.024	-17.32	363.83	55.22	6.59	0.886	0.800	0.023	0.030	-0.453
-20	-40	1.512	0.626	2.416	-18.92	612.54	56.95	10.75	0.923	0.765	0.024	0.021	-0.459
-20	-30	1.512	0.993	1.522	-19.76	985.69	42.29	23.31	0.959	0.733	0.020	0.014	-0.463
-10	-50	2.221	0.376	5.910	-7.56	334.00	71.31	4.68	0.840	0.893	0.066	0.065	-0.461
-10	-40	2.221	0.626	3.549	-9.16	564.51	82.67	6.83	0.879	0.851	0.064	0.055	-0.465
-10	-30	2.221	0.993	2.236	-9.99	911.64	81.83	11.14	0.917	0.812	0.059	0.057	-0.458
-10	-20	2.221	1.512	1.469	-10.00	1416.05	58.68	24.13	0.954	0.777	0.050	0.045	-0.467
0	-40	3.161	0.626	5.051	0.25	515.25	106.64	4.83	0.829	0.956	0.114	0.100	-0.469
0	-30	3.161	0.993	3.183	0.00	835.67	118.61	7.05	0.870	0.909	0.106	0.091	-0.471
0	-20	3.161	1.512	2.090	0.00	1303.14	113.35	11.50	0.909	0.866	0.095	0.087	-0.469
0	-10	3.161	2.221	1.423	0.00	1965.18	78.78	24.94	0.948	0.828	0.080	0.067	-0.486
10	-40	4.377	0.626	6.995	10.00	464.64	128.90	3.60	0.774	1.089	0.176	0.156	-0.475
10	-30	4.377	0.993	4.408	10.00	757.65	152.75	4.96	0.816	1.030	0.164	0.140	-0.479
10	-20	4.377	1.512	2.895	10.00	1187.17	164.01	7.24	0.858	0.977	0.149	0.124	-0.486
10	-10	4.377	2.221	1.971	10.00	1798.06	152.04	11.83	0.899	0.929	0.131	0.108	-0.495
10	0	4.377	3.161	1.385	10.00	2645.61	103.05	25.67	0.940	0.887	0.109	0.095	-0.504
20	-40	5.918	0.626	9.458	20.00	412.59	149.52	2.76	0.711	1.262	0.256	0.228	-0.482
20	-30	5.918	0.993	5.959	20.00	677.39	184.37	3.67	0.756	1.185	0.237	0.205	-0.487
20	-20	5.918	1.512	3.914	20.00	1067.88	210.83	5.07	0.801	1.117	0.217	0.174	-0.503
20	-10	5.918	2.221	2.665	20.00	1626.14	219.64	7.40	0.845	1.057	0.195	0.155	-0.510
20	0	5.918	3.161	1.872	20.00	2404.18	198.52	12.11	0.887	1.004	0.169	0.144	-0.514
20	10	5.918	4.377	1.352	20.00	3466.38	131.71	26.32	0.930	0.957	0.137	0.114	-0.540
30	-40	7.835	0.626	12.521	30.00	358.93	168.47	2.13	0.640	1.495	0.362	0.321	-0.494
30	-30	7.835	0.993	7.889	30.00	594.65	213.41	2.79	0.688	1.391	0.334	0.283	-0.504
30	-20	7.835	1.512	5.182	30.00	944.89	253.99	3.72	0.735	1.302	0.306	0.250	-0.514
30	-10	7.835	2.221	3.528	30.00	1448.91	281.84	5.14	0.782	1.223	0.277	0.218	-0.528
30	0	7.835	3.161	2.479	30.00	2155.28	286.22	7.53	0.827	1.155	0.245	0.190	-0.542
30	10	7.835	4.377	1.790	30.00	3124.24	253.00	12.35	0.873	1.095	0.209	0.163	-0.561
30	20	7.835	5.918	1.324	30.00	4431.45	165.16	26.83	0.916	1.043	0.167	0.142	-0.579
40	-40	10.183	0.626	16.272	40.00	303.42	185.82	1.63	0.561	1.829	0.512	0.454	-0.509
40	-30	10.183	0.993	10.253	40.00	509.06	239.98	2.12	0.611	1.681	0.467	0.396	-0.521
40	-20	10.183	1.512	6.734	40.00	817.68	293.40	2.79	0.661	1.556	0.425	0.344	-0.537
40	-10	10.183	2.221	4.585	40.00	1265.58	338.89	3.73	0.710	1.449	0.385	0.302	-0.550
40	0	10.183	3.161	3.222	40.00	1897.83	366.51	5.18	0.759	1.357	0.345	0.262	-0.568
40	10	10.183	4.377	2.326	40.00	2770.34	364.33	7.60	0.806	1.277	0.302	0.232	-0.583
40	20	10.183	5.918	1.721	40.00	3953.34	316.23	12.50	0.853	1.209	0.254	0.193	-0.613
40	30	10.183	7.835	1.300	40.00	5535.95	203.11	27.26	0.900	1.151	0.200	0.162	-0.644
50	-40	13.021	0.626	20.808	50.00	245.70	201.61	1.22	0.471	2.349	0.740	0.659	-0.527

50	-30	13.021	0.993	13.111	50.00	420.07	264.21	1.59	0.523	2.118	0.663	0.570	-0.540
50	-20	13.021	1.512	8.611	50.00	685.41	329.32	2.08	0.576	1.930	0.597	0.491	-0.558
50	-10	13.021	2.221	5.863	50.00	1074.96	390.66	2.75	0.628	1.773	0.538	0.424	-0.576
50	0	13.021	3.161	4.119	50.00	1630.14	439.74	3.71	0.679	1.642	0.482	0.371	-0.593
50	10	13.021	4.377	2.975	50.00	2402.37	465.48	5.16	0.729	1.532	0.428	0.320	-0.616
50	20	13.021	5.918	2.200	50.00	3456.22	454.19	7.61	0.779	1.438	0.371	0.277	-0.641
50	30	13.021	7.835	1.662	50.00	4873.33	388.75	12.54	0.827	1.360	0.310	0.241	-0.671
50	40	13.021	10.183	1.279	50.00	6760.67	246.83	27.39	0.875	1.294	0.238	0.202	-0.716

The table indicates that HFO-1234yf has less pressure ratio and discharge temperature than R134a, which is an advantage, but it has less COP_{2d} and Carnot efficiency which is a disadvantage. See [1] for R134a cycle data. At t_1 = 40 °C and t_2 = -10 and 10 °C, HFO-1234yf has a pressure ratio less by 9.5% and 5.1%, and discharge temperature by 6.3 and 3.1°C, respectively. At t_1 = 40 °C and t_2 = -10 and 10 °C, HFO-1234yf has less COP_{2d} by -7.4% and 4.5% and η_{cd} by 7.3% and 4.4%, respectively. The table also indicates that HFO-1234yf is significantly more influenced by subcooling and superheating than R134a. At t_1 = 40 °C and t_2 = -10 and 10 °C, HFO-1234yf has higher y_1 and y_2 by nearly 30% and 250%.

Pressure drop and heat transfer in plate heat exchangers

Pressure drop and heat transfer in the evaporator and condenser may be predicted if all the transport properties of the refrigerant and the secondary coolants, mass flow rates, and the construction of the heat exchangers are known. If adequate information is not available or a general prediction is needed, a comparison between refrigerants' performances under the same conditions may be used. This can be done by separating the independent properties of the refrigerant in correlations for pressure drop and heat transfer to form what is called figures of merit.

To compare the pressure drop in the evaporator with HFO-1234yf to R134a, Blasius correlation for pressure drop in turbulent single phase may be used. According to this correlation $\Delta p = f1\frac{\rho w^2}{2}\cdot\frac{L}{d}$, where f_1 =0.316 $Re^{-0.25}$

Substitute the velocity in terms of the mass flow rate m_r, and then m_r in terms of Q_2/h_{fg}, the Blasius equation for different refrigerants and similar Q_2, L, and d yields:

$\Delta p = const\times\frac{\mu^{0.25}}{\rho h_{fg}^{1.75}}$ = *const* x $FOM_{\Delta p}$, where $FOM_{\Delta p}$ is figure of merit for pressure drop.

Figure of merit for heat transfer may be calculated using Dittus-Boelter equation for turbulent single phase heat transfer:

$Nu = 0.023\ Re^{0.8}\ Pr^{0.4}$ which yields,

$FOM_{SPHT} = k Pr^{0.4}/(h_{fg}\mu)^{0.8}$

Boiling figure of merit may be derived from Cooper's pool boiling correlation:

$H_{pb} = 55\ p_{red}^{0.12-0.2\log_{10}Rp}(-\log_{10}p_{red})^{-0.55}M^{-0.5}q^{0.67}$

Taking the surface roughness R_p as 1μm, the figure of merit for boiling will be

$FOM_{pb} = p_{red}^{0.12}(-\log_{10}p_{red})^{-0.55}M^{-0.5}$

Condensation figure of merit can be derived from Nusselt's film theory applied for laminar condensation in vertical tube.

Average condensation heat transfer h_c = const $(k_l^3\ \rho_l(\rho_l - \rho_g)/\mu_l\ \Gamma_l)^{1/3}$, where Γ_l is the condensation rate at length l divided by the inside tube circumference. $\Gamma_l = Q_{cond}/h_{fg}\ \pi d_i$

Substitute this value into the equation of the heat transfer coefficient and consider ρ_lNNρ_g and Q_{cond} constant for the two compared refrigerants:

h_c = const $k_l\ (\rho_l^2\ h_{fg}/\mu_l)^{1/3}$ = const FOM_{cond}

Ratio of the pressure drops and the heat transfer coefficients of HFO-1234yf and R134a may be predicted by dividing their relevant figures of merit. Figure of merit for pressure drop is calculated for vapor. The tables below present the calculated data.

Table 3 Evaporator figures of merit

	HFO-1234yf				R134a			
T_2 (°C)	$FOM_{\Delta p}$	FOM_{SPHT} liquid	FOM_{SPHT} vapor	FOM_{pb}	$FOM_{\Delta p}$	FOM_{SPHT} liquid	FOM_{SPHT} vapor	FOM_{pb}
-20	2.44E-05	0.02647	0.02618	0.05469	2.21E-05	0.02336	0.01983	0.05283
-10	1.81E-05	0.02817	0.02804	0.06159	1.6E-05	0.02480	0.02148	0.05958
-5	1.58E-05	0.02907	0.02905	0.06534	1.37E-05	0.02555	0.02237	0.06325
0	1.39E-05	0.03001	0.03013	0.06935	1.19E-05	0.02634	0.02330	0.06713
5	1.23E-05	0.03100	0.03128	0.07363	1.05E-05	0.02716	0.02429	0.07126
10	1.1E-05	0.03204	0.03251	0.07822	9.22E-06	0.02803	0.02534	0.07567
15	9.85E-06	0.03316	0.03384	0.08317	8.19E-06	0.02895	0.02648	0.08040
20	8.91E-06	0.03435	0.03529	0.08854	7.33E-06	0.02993	0.02770	0.08550

Table 4 Calculated ratios of pressure drops and heat transfer coefficients of HFO-1234yf to R134a for similar evaporating effects

T_2 (°C)	Δp ratio	h_{Liquid} ratio	h_{Vapor} ratio	h_{pb} ratio
-20	1.106	1.133	1.321	1.035
-10	1.136	1.136	1.306	1.034
-5	1.150	1.138	1.299	1.033
0	1.164	1.139	1.293	1.033
5	1.177	1.141	1.288	1.033
10	1.190	1.143	1.283	1.034
15	1.203	1.145	1.278	1.034
20	1.216	1.148	1.274	1.036

Table 5 Condenser figures of merit

T_1(°C)	HFO-1234yf FOMcond	R134a FOMcond	h_{fc} ratio
40	6475.151	8208.119	0.78887
50	6055.905	7685.111	0.78800

Experimental data

A refrigeration rig with R134a and a maximum cooling capacity of 3kW is used as a drop-in unit. It has a plate evaporator that is heated by a controlled brine loop, and a plate condenser with water as a secondary coolant. Tests were run, firstly with R134a followed by HFO-1234yf, at condenser temperature of 41°C and evaporating temperature ranging between -8 and 16. Overall heat transfer coefficient for the condenser is estimated only for saturation condition while for evaporator a little superheat was considered. Results of the experimental work are presented in the figures and tables below.

Table 6 R134a experimental data

p_1	T_{1sat}	$T_{1(in)}$	$T_{1(out)}$	$p_{2(in)}$	$p_{2(out)}$	Δp_2	$T_{2sat(in)}$	T_{exp}	$T_{2(out)}$	$T_{w(in)}$	$T_{w(out)}$	m_w (kg/s)	$T_{b(in)}$	$T_{b(out)}$	m_r (kg/s)	$Q_{2(in)}$ (kW)
10.4	40.851	72.4	27.7	2.2	2.186	0.01413	-7.638	26.3	-6.7	16.6	40.7	0.01314	-0.8	-3.7	0.00641	0.821
10.6	41.567	64.3	35	3.55	3.522	0.02783	5.437	28.6	8	15.8	40.8	0.02101	14	10.8	0.01073	1.699
10.6	41.567	60.3	35.8	4.9	4.858	0.04220	15.104	33.4	20.4	15.1	40.6	0.02830	25.3	21.3	0.01557	2.457

Table 7 HFO-1234yf experimental data

p_1	T_{1sat}	$T_{1(in)}$	$T_{1(out)}$	$p_{2(in)}$	$p_{2(out)}$	Δp_2	$T_{2sat(in)}$	T_{exp}	$T_{2(out)}$	$T_{w(in)}$	$T_{w(out)}$	m_w (kg/s)	$T_{b(in)}$	$T_{b(out)}$	m_r (kg/s)	$Q_{2(in)}$ (kW)
10.5	41.213	64.2	28.3	2.4	2.383	0.01734	-7.872	27.3	-2.6	16.2	40.7	0.01314	-0.3	-3	0.00788	0.797
10.6	41.591	57.8	35.1	3.95	3.912	0.03758	6.760	32.2	13.5	15.1	40.3	0.02134	15.4	12.4	0.01389	1.638
10.6	41.591	55.9	32	5.22	5.168	0.05180	15.746	32.2	23.5	14.7	39.6	0.02844	26.3	22.3	0.01842	2.400

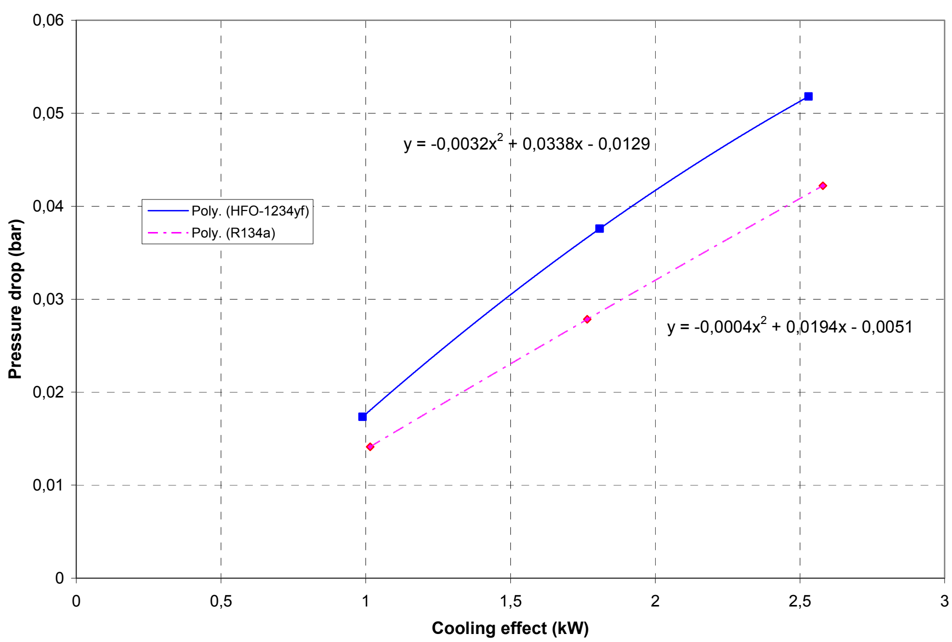

Fig. 4 Evaporator pressure drop

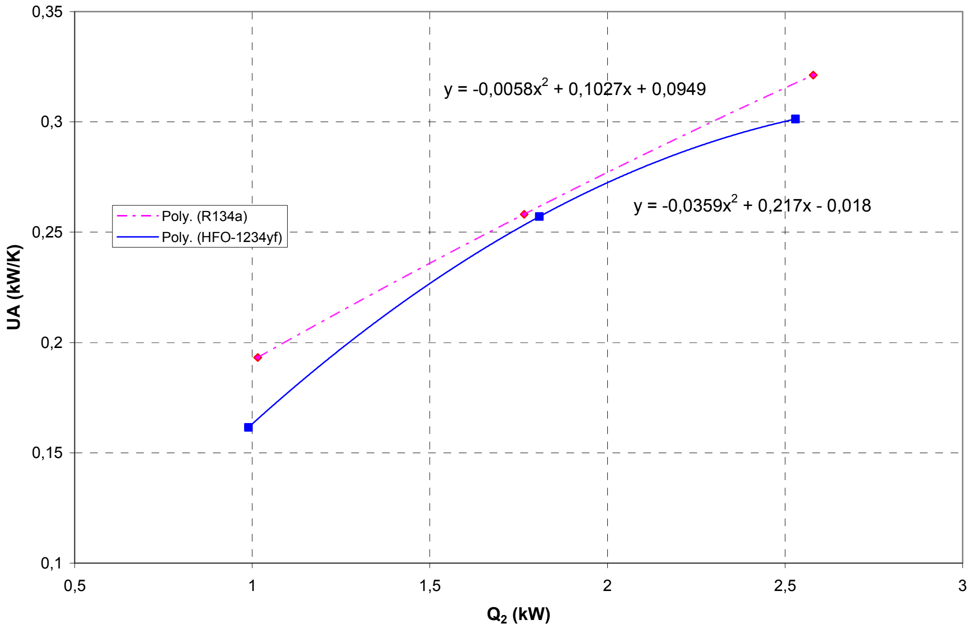

Fig. 5 Evaporator heat transfer

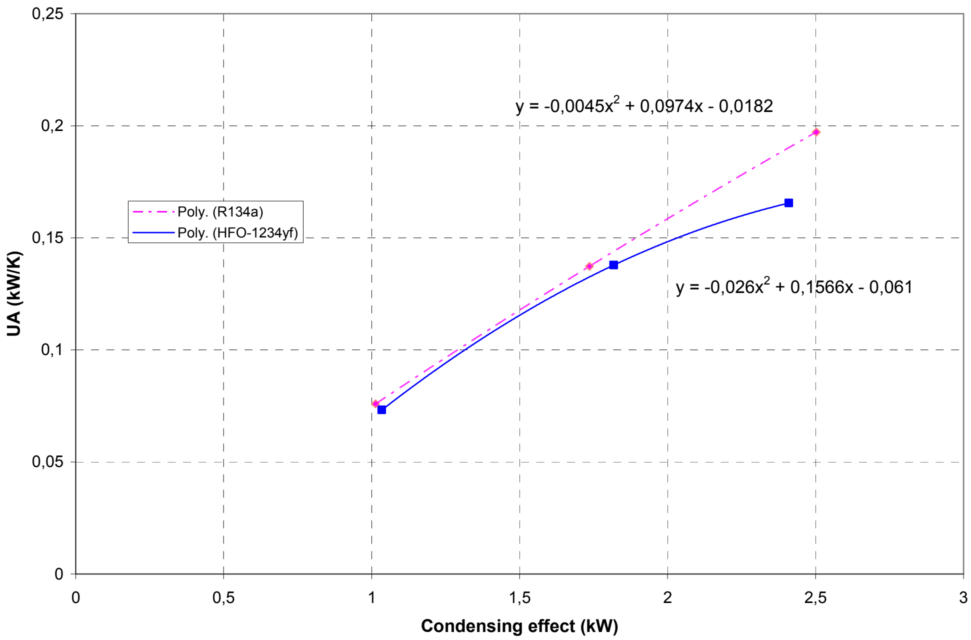

Fig. 6 Condenser heat transfer

Table 8 Evaporator experimental results at t_1 = 41°C

Q_2 (kW)	Δp_{R134a} (bar)	$\Delta p_{R1234yf}$ (bar)	UA_{R134a} (kW/K)	$UA_{R1234yf}$ (kW/K)	*Δp* ratio	*UA* ratio
1	0.0135	0.0177	0.1918	0.1631	1.311	0.850
1.5	0.0225	0.0306	0.2359	0.2267	1.360	0.961
2.5	0.0399	0.0516	0.3154	0.3001	1.293	0.952

Table 9 Condenser experimental results at t_1 = 41°C

Condensing effect **(kW)**	UA_{R134a} **(kW/K)**	$UA_{R1234yf}$ **(kW/K)**	***UA ratio***
1.4	0.109	0.107	0.981
1.9	0.151	0.143	0.947
2.9	0.226	0.174	0.771

Discussion of results

Experimental results show that HFO-1234yf has higher pressure drop and lower heat transfer coefficient than those predicted, particularly at lower evaporating temperature. This is due to the higher superheat encountered at these temperatures which accelerates the refrigerant and practically decreases the boiling heat transfer area. Condenser data show that HFO-1234yf gives less increment in heat transfer coefficient than R134a at higher heat capacity. This can be explained by the fact that the theoretical prediction is based only on a film condensation correlation, ignoring by that the convective heat transfer contribution. At significant condenser heat rejection the higher refrigerant mass flow rate induces greater convective heat transfer, and since the two refrigerants have different properties related to the convective heat transfer, the variations of their overall heat transfer coefficients with condenser effects will be different.

Suggestions for future work

Acquire more compressor data with the new refrigerants to investigate the practical *COP* of the refrigeration system and the efficiencies and reliability of the compressor.

References

1. Eric Granryd, Ingvar Ekroth, Per Lundqvist, Åke Melinder, Björn Palm, Peter Rohlin “Refrigerating Engineering” KTH, Energiteknik, Stockholm Sweden
2. RefProp: fluid thermodynamic and transport properties NIST, version 7
3. Björn Palm “Hydrocarbons as refrigerants in small heat pump and refrigeration systems” *Direct Science*, available on line at: www.sciencedirect.com
4. Thomas J. Leck, PhD ”Development and Evaluation of High Performance, Low GWP Refrigerants for AC and Refrogeratopn” Dul,Pont Fluorochemicals R&D, Wilmington, Delaware, 19880,USA